

## Supramolecular Chemistry | Hot Paper |

## Influence of Ester versus Amide Linkers on the Supramolecular Polymerization Mechanisms of Planar BODIPY Dyes

Alexander Rödle,<sup>[a, b]</sup> Benedikt Ritschel,<sup>[b]</sup> Christian Mück-Lichtenfeld,<sup>[a]</sup>  
Vladimir Stepanenko,<sup>[b]</sup> and Gustavo Fernández\*<sup>[a, b]</sup>

**Abstract:** We report the H-type supramolecular polymerization of two new hydrophobic BODIPY derivatives equipped with ester and amide linkages. Whereas the ester-containing BODIPY derivative undergoes an isodesmic supramolecular polymerization in which the monomers are parallel-oriented, the replacement of the ester by amide groups leads to a highly cooperative self-assembly process into H-

type aggregates with a rotational displacement of the dye molecules within the stack. The dye organization imposed by simultaneous  $\pi$ - $\pi$  and hydrogen bonding interactions is the driving force for the cooperative supramolecular polymerization, whereas the absence of additional hydrogen bonds for the ester-containing moiety does not suffice to induce cooperative phenomena.

## Introduction

The phenomenon of self-assembly has been extensively studied over the last decades with the main goal of providing access to functional materials.<sup>[1]</sup> The molecular organization correlates with the specific intermolecular interactions during the supramolecular polymerization process and is more amenable to detailed research when using one-dimensional systems.<sup>[2]</sup> In this regard, hierarchical supramolecular structures that follow a cooperative self-assembly mechanism are desirable due to their higher degree of internal order compared to non-cooperative counterparts.<sup>[3]</sup> The exploitation of cooperative hydrogen bonds based on functional groups such as ureas,<sup>[4]</sup> bisureas,<sup>[5]</sup> amides,<sup>[6]</sup> bisamides,<sup>[7]</sup> melamines<sup>[8]</sup> and peptides<sup>[9]</sup> often reinforced by  $\pi$ - $\pi$  interactions<sup>[10]</sup> is a well-known strategy to fine tune the aggregation modes and in turn, the degree of order in these systems. In sharp contrast, the direct influence of ester linkages on supramolecular polymerization mechanisms remain thus far unexplored, despite the fact that ester functionalities are commonly used, synthetically accessible building blocks in self-assembled structures<sup>[11]</sup> and liquid crystals.<sup>[12]</sup> Recently, the influence of the linking group (ester vs. amide) on the self-assembly and gelation of *trans*-bis(pyridine) dichloroplatinum(II) complexes has been studied.<sup>[13]</sup> Although the molecular packing is strongly biased by the exist-

ence of a sterically hindered Pt<sup>II</sup> center, a clear transition from J- to H-type aggregates is observed when replacing the ester by the amide moiety, thus showing the potential of these linkers.

We envisaged that a planar  $\pi$ -system without any sterically demanding groups would represent an ideal building block to directly analyze the influence of ester versus amide groups on aggregation mechanisms. To this end, we have selected a 4,4-difluoro-4-bora-3a,4a-diaza-s-indacene (BODIPY)<sup>[14]</sup> core not only for its small size and planarity but also due to its well-known ability to self-assemble in an H-<sup>[15]</sup> or J-type<sup>[16]</sup> fashion, which can be readily investigated by common spectroscopic methods.

For instance, our group has recently described the self-assembly of rod-like hydrophobic<sup>[17]</sup> and amphiphilic BODIPY dyes<sup>[18]</sup> as well as the ability of the latter to encapsulate hydrophobic dye molecules in aqueous media.<sup>[18]</sup> The self-assembly of these systems is primarily driven by  $\pi$ - $\pi$  interactions of the dipyrromethane core, leading in most cases to an isodesmic (non-cooperative) supramolecular polymerization due to the absence of supportive noncovalent forces. In this work, we examine whether the self-assembly mechanism of BODIPY dyes can be tuned by introducing ester or amide groups that can eventually reinforce the stacking of the BODIPY units by additional noncovalent interactions.

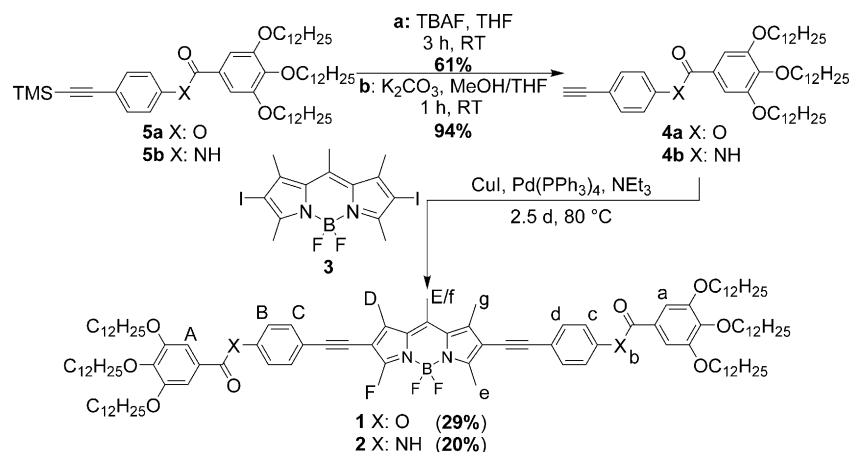
## Results and Discussion

The target ester- (1; Scheme 1) and amide-containing (2) BODIPY derivatives are readily obtained in moderate to good yields by modified literature procedures.<sup>[17,19]</sup> Previously described 4-iodophenyl-3,4,5-tris(dodecyloxy)benzoate<sup>[19d]</sup> and 3,4,5-tris(dodecyloxy)-N-(4-iodophenyl)benzamide<sup>[19c]</sup> were used as starting materials for the synthesis of compounds **5a** and **5b** through a Sonogashira reaction in the presence of trime-

[a] A. Rödle, Dr. C. Mück-Lichtenfeld, Prof. Dr. G. Fernández  
Organisch-Chemisches Institut, Westfälische Wilhelms-Universität Münster  
Corrensstraße 40, 48149 Münster (Germany)  
E-mail: fernandg@uni-muenster.de

[b] A. Rödle, B. Ritschel, Dr. V. Stepanenko, Prof. Dr. G. Fernández  
Institut für Organische Chemie and Center for Nanosystems Chemistry  
Julius-Maximilians-Universität Würzburg  
Am Hubland, 97074 Würzburg (Germany)

Supporting information for this article is available on the WWW under  
<http://dx.doi.org/10.1002/chem.201602592>.



**Scheme 1.** Synthesis route towards BODIPY compounds **1** and **2**.

thylsilylacetylene (TMS). Further deprotection of the TMS group was carried out following two different procedures. The amide derivative was converted to **4b** by using  $K_2CO_3$  in a mixture of THF/MeOH, whereas for the ester compound less nucleophilic conditions were chosen, as a result of the lower stability of the ester functionality, using tetra-*n*-butylammonium fluoride (TBAF) in THF yielding **4a**. Finally, a Sonogashira reaction using CuI, Pd(PPh<sub>3</sub>)<sub>4</sub> in NEt<sub>3</sub> with the diiodo BODIPY derivative **3**<sup>[17]</sup> was carried out to synthesize the final compounds **1** and **2**. Both molecules were fully characterized by <sup>1</sup>H/<sup>13</sup>C NMR spectroscopy, HRMS and elemental analysis.

Initial comparison between the self-assembly behavior of **1** and **2** was provided by complementary UV/Vis and fluorescence studies. Nevertheless, due to the differing nature of the linking groups (ester vs. amide) both molecules (**1** and **2**) show differences in their solubility, solvent-dependent UV/Vis and fluorescence spectra. Figure 1a shows the absorption spectra of **1** in different solvents ( $c=1 \times 10^{-4}$  M) at room temperature (RT).

These experiments show minor spectral changes exhibiting a collective maximum at  $\approx 569$  nm, which is assigned to the  $S_0 \rightarrow S_1$  ( $\pi-\pi^*$ ) transition of the BODIPY chromophore, whereas the  $S_0 \rightarrow S_2$  transition appears in the region around 400 nm (Figure S11 in the Supporting Information).<sup>[20]</sup> By contrast, the absorption spectra in methylcyclohexane (MCH) (Figure 1a) and other selected aliphatic solvents, such as cyclohexane and *n*-hexane (Figure S11), show a blue-shifted shoulder at 539 nm that appears in addition to the maximum at 567 nm. These observations suggest the initial stages of an H-type aggregation phenomenon that takes place exclusively in aliphatic solvents (cyclohexane, *n*-hexane and MCH) from among all investigated solvents (Figure S11). Due to a comparable self-assembly behavior in these media, we have restricted ourselves to MCH for further studies due to its higher solubility and boiling point compared to hexane and cyclohexane. In analogy to UV/Vis spectroscopy, solvent-dependent fluorescence experiments of **1** were carried out at RT (Figure 1b). The curve progression, relative intensities as well as the position of the maxima (593 nm) are similar in most investigated solvents. A somewhat

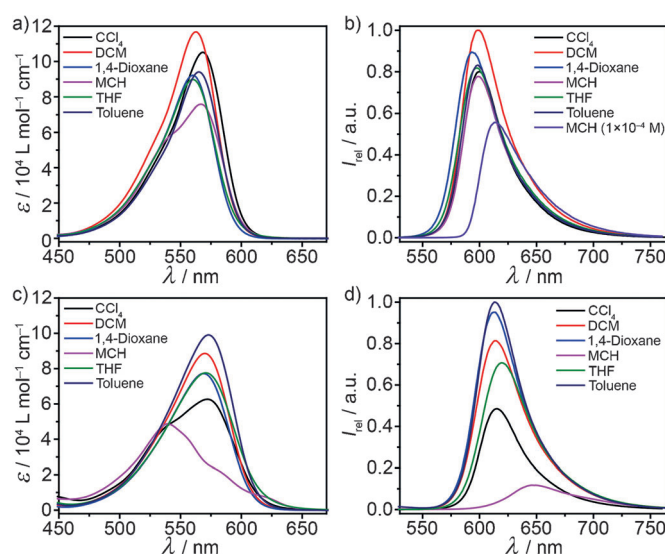


**Figure 1.** Solvent-dependent fluorescence studies of: a) **1** ( $\lambda_{ex}=500$  nm,  $c=1 \times 10^{-5}$  M), and c) **2** ( $\lambda_{ex}=440$  nm,  $c=1 \times 10^{-5}$  M) at RT; and solvent-dependent UV/Vis spectroscopy of: b) **1** ( $c=1 \times 10^{-4}$  M), and d) **2** ( $c=1 \times 10^{-5}$  M).

different behavior is observed in a selected nonpolar solvent (MCH) at a slightly higher concentration ( $c=10^{-4}$  M) wherein a red-shift to 614 nm and a decrease in the fluorescence intensity can be noticed (Figure 1b). Slightly different optical properties are observed for the amide-substituted BODIPY derivative **2**. For instance, the majority of the absorption spectra feature a common maximum at 573 nm (Figure 1c). In contrast, a hypsochromic shift ( $\Delta\lambda=34$  nm) of the absorption spectrum in MCH and cyclohexane can be noticed (Figure 1c and Figure S14). This effect is even more pronounced in hexane (Figure S14), however due to the limited solubility of **2** in this medium, this solvent was not considered for further investigations. These findings are in line with solvent-dependent fluorescence studies. The majority of the fluorescence spectra feature a common maximum at 613 nm. In contrast, a bathochromic shift ( $\Delta\lambda=34$  nm) of the absorption spectrum in MCH and

a dramatically reduced emission intensity ( $\approx 90\%$ ) can be noticed (Figure 1d). The observations extracted from absorption and emission studies indicate a supramolecular polymerization with an H-type excitonic coupling of the dye molecules.<sup>[21]</sup> An interesting spectral feature that is worth mentioning is the appearance of a red-shifted shoulder at 620 nm in the aggregate spectrum of the amide-containing BODIPY dye **2** (Figure 1c) that is absent in the aggregate spectrum of the ester-containing system **1** even at millimolar concentration (Figure 2a). This appreciable difference points to a different dye arrangement in both systems.

To investigate the process of self-aggregation in detail, temperature- and concentration-dependent spectroscopic measurements are powerful tools. Due to the higher solubility and reduced aggregation propensity of **1**, its supramolecular polymerization was analyzed by concentration-dependent UV/Vis and fluorescence experiments, whereas related temperature-dependent investigations are necessary for **2** in order to identify the monomer species. Figure 2a depicts the concentration-dependent UV/Vis studies of **1** in MCH between  $5.09 \times 10^{-3}$  and  $2.20 \times 10^{-6}$  M at RT. On increasing the concentration, the previously described monomer band (569 nm) decays in favor of a transition at 539 nm corresponding to the self-assembled species. The isosbestic points at 548 and 603 nm indicate an equilibrium between the monomeric and aggregated species. In order to inspect the supramolecular polymerization mechanism, the molar absorptivity at 569 nm of this transition process was monitored against concentration (Figure 2c). The resulting sigmoidal curve can be suitably fitted to the concentration-dependent isodesmic aggregation model (Figure 2c),<sup>[11]</sup> obtaining a binding constant  $K$  of  $6.6 \times 10^3 \text{ M}^{-1}$  (Table 1). The concentration-dependent fluorescence studies of **1** in MCH (Figure 2b and Figure S13 in the Supporting Information) show that an increase in concentration ( $1 \times 10^{-5}$ – $1 \times 10^{-3}$  M) induces a steady red shift and decrease in the emission intensity, which is in accordance with the results obtained by UV/Vis experiments and demonstrates a face-to-face H-type stacking of the dyes within the aggregate.

On the other hand, the aggregation behavior of **2** is slightly different. For this dye, temperature-dependent studies appeared to be the most suitable experiments for analyzing in detail the spectral changes, as dilution experiments are not sufficient for reaching a fully monomeric state. Figure 2d shows the impact of a temperature decrease (90–25 °C) on the

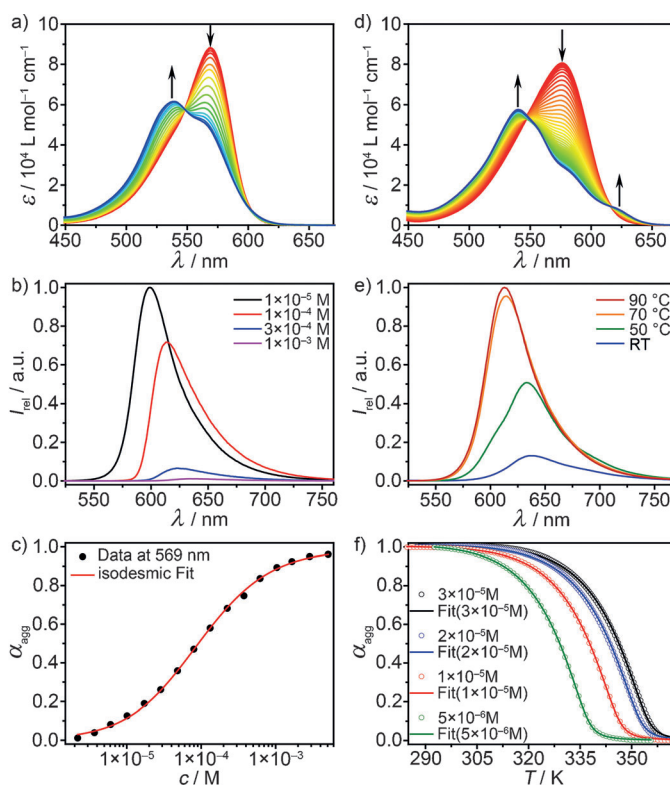


**Figure 2.** a) Concentration-dependent UV/Vis studies of **1** ( $5.09 \times 10^{-3}$  to  $2.20 \times 10^{-6}$  M, MCH), and b) concentration-dependent fluorescence spectroscopy of **1** ( $1 \times 10^{-6}$ – $1 \times 10^{-3}$  M, MCH) at RT. c) Fit of the data of the absorption experiments of **1** to the isodesmic model ( $\alpha_{\text{agg}}$  vs.  $\log[c]$ , 569 nm). d) Temperature-dependent UV/Vis experiments of **2** ( $c = 1 \times 10^{-5}$  M, MCH), and e) temperature-dependent fluorescence spectroscopy of **2** ( $c = 1 \times 10^{-5}$  M, MCH) between 365 and 285 K. f) Cooling curves ( $\alpha_{\text{agg}}$  vs.  $T$ ) obtained by monitoring the absorption of **2** at 576 nm versus  $T$  at different concentrations ( $5 \times 10^{-6}$ – $3 \times 10^{-5}$  M) and fits to the nucleation–elongation model. The arrows in (a) and (d) indicate the spectral changes with increasing concentration and decreasing temperature, respectively.

UV/Vis absorption spectra of **2** in MCH at a concentration of  $1 \times 10^{-5}$  M. On cooling, the depletion of the absorption maximum at 576 nm is concomitant with the rise of a blue-shifted aggregate band at 540 nm (Figure 2d). The existence of two isosbestic points at 548 and 616 nm is indicative of an equilibrium between monomeric and H-type species. Temperature-dependent fluorescence spectroscopy of **2** ( $c = 1 \times 10^{-5}$  M) in MCH (Figure 2e) shows both a red-shift and quenching of the emis-

Table 1. Thermodynamic parameters associated to the self-assembly of <b>1</b> and <b>2</b> in MCH. <sup>[a]</sup>							
Compound	$\lambda$ [nm]			$K$ [ $\text{M}^{-1}$ ]	$-\Delta G_{298}$ [ $\text{kJ mol}^{-1}$ ]		
<b>1</b>	569			$6579.7 \pm 257.7$	21.8		
$C(2)$ [M]	$\Delta H_{\text{nucl}}^0$ [ $\text{kJ mol}^{-1}$ ]	$\Delta H^0$ [ $\text{kJ mol}^{-1}$ ]	$\Delta S^0$ [ $\text{kJ mol}^{-1} \text{K}^{-1}$ ]	$T_e$ [K]	$K_{\text{nucl}}$ [ $\text{M}^{-1}$ ]	$K_{\text{el}}$ [ $\text{M}^{-1}$ ]	$\sigma$
$1.0 \times 10^{-5}$	$-15.0 \pm 0.2$	$-85.3 \pm 0.5$	$-0.1516 \pm 0.0014$	$344.8 \pm 0.07$	$5.3 \times 10^2$	$1.0 \times 10^5$	$5.3 \times 10^{-3}$

[a]  $K$  = equilibrium constant;  $-\Delta G_{298}$  = standard Gibbs free energy;  $\Delta H_{\text{nucl}}^0$  = nucleation enthalpy;  $\Delta H^0$  = enthalpy difference;  $\Delta S^0$  = entropy difference;  $T_e$  = elongation temperature;  $K_{\text{nucl}}$  = equilibrium constant of the nucleation process;  $K_{\text{el}}$  = equilibrium constant of the elongation process;  $\sigma$  = degree of cooperativity ( $K_{\text{nucl}}/K_{\text{el}}$ ).

sion spectra upon cooling from 90 °C to RT, which supports the formation of an H-type supramolecular polymer.

In order to understand the specific process in more detail, cooling curves of **2** (cooling rate = 1 K min<sup>-1</sup>) extracted from temperature-dependent UV/Vis studies in MCH at different concentrations were measured, as shown in Figure 2f. Each cooling curve could be perfectly fitted to the cooperative nucleation–elongation model.<sup>[22]</sup> The thermodynamic parameters are shown in Table 1 and Table S1 in the Supporting Information. The high binding constants of the supramolecular elongation step (up to 2.0 × 10<sup>5</sup> M<sup>-1</sup>), which is around three times higher than the *K* value of **1**, along with the low  $\sigma$  values (between 4.8 × 10<sup>-3</sup> and 5.7 × 10<sup>-3</sup>) correspond to a cooperative self-aggregation process. By comparing the self-assembly behavior as well as the supramolecular polymerization mechanism, one can notice significant differences between **1** and **2**. In order to understand this dissimilarity, the reason for it has to lie on the molecular level, since the linking group is the only difference between both molecules. An amide group is, in contrast to the ester linker, both a hydrogen bond acceptor and donor, which provides an additional intermolecular force. The UV/Vis spectra of **2** are reminiscent of the H-type aggregates reported by the Würthner group<sup>[23]</sup> and us<sup>[18]</sup> in terms of a blue-shifted transition as well as a red-shifted shoulder relative to the monomer spectrum. The blue-shifted peak at 520 nm indicates a face-to-face H-type stacking whereas the red-shifted shoulder at 620 nm correlates with a rotational displacement of the BODIPY chromophores in the stack.<sup>[21]</sup> Thus, to provide intermolecular hydrogen bonds between the amide groups, the molecules undergo a rotational face-to-face stacking on the account of the grade of the  $\pi$ - $\pi$  stacking's overlap. In sharp contrast ester-containing BODIPY **1** shows also a blue-shift in the spectra but no red-shifted shoulder, which indicates that the rotational displacement becomes less prominent for this system. Ultimately, the additional intermolecular force assisting hydrogen bonding tunes the isodesmic to a cooperative H-type self-aggregation process.

To investigate the participating intermolecular forces during the aggregation process in more detail, concentration-dependent <sup>1</sup>H NMR measurements were recorded. A concentration-dependent shift of the proton signals in the NMR spectrum indicates participation of the very same during the supramolecular polymerization process, caused by a change of the spatial environment of the particular protons. For instance, the shielding of the aromatic protons is commonly attributed to the  $\pi$ - $\pi$  stacking of the aromatic planes whereas hydrogen-bond interactions usually cause a downfield shift of the involved proton NMR signals.<sup>[24]</sup> For the target systems **1** and **2**, concentration-dependent <sup>1</sup>H NMR measurements were recorded (Figure 3).

Upon increasing the concentration of **1** ([D<sub>14</sub>]MCH, Figure 3a), both proton signals of the aromatic plane (H<sub>A</sub>, H<sub>B</sub> and H<sub>C</sub>) and those of the methyl groups of the BODIPY core (H<sub>D</sub>, H<sub>E</sub> and H<sub>F</sub>) undergo upfield shifts, thus supporting  $\pi$ - $\pi$  stacking of the molecules (for proton labeling see Scheme 1; capital letters **1**, small letters **2**). A similar shielding effect upon cooling a solution of **1** from 343 K to RT was observed by temperature-dependent <sup>1</sup>H NMR experiments (17.5 mm, 600 MHz; Fig-

ure S20 in the Supporting Information). By monitoring chemical shifts of proton H<sub>A</sub> versus concentration, a sigmoidal aggregation curve was observed and fitted to the isodesmic model (Figure S21).

We next attempted to analyze the influence of temperature on the chemical shifts of **2** in [D<sub>14</sub>]MCH, as it was previously observed that temperature-dependent spectroscopic studies worked well for this system. However, the stronger tendency of **2** to self-assemble compared to **1** leads to a severe broadening of the proton NMR signals even at elevated temperatures. Thus, the selection of a more appropriate solvent mixture was required in order to monitor the self-assembly of **2** through NMR spectroscopy experiments. CD<sub>2</sub>Cl<sub>2</sub> was the first solvent of choice, however, the good solvation of the units of **2** in this solvent, results in minor changes in the chemical shifts upon increasing concentration. In order to find the right conditions providing the balance between both a strong tendency to aggregate and a sufficient solubility, we selected CCl<sub>4</sub> as a “poor solvent” in combination with CD<sub>2</sub>Cl<sub>2</sub>. Previous UV/Vis and fluorescence results (Figure 1c and d) had suggested the initial stages of a self-assembly process in this solvent. However, this was not as strong as in hydrocarbon solvents. By mixing CD<sub>2</sub>Cl<sub>2</sub> and CCl<sub>4</sub> in different ratios, we found that the solvent mixture CCl<sub>4</sub>/CD<sub>2</sub>Cl<sub>2</sub> (9:1, v/v) was the most appropriate one in

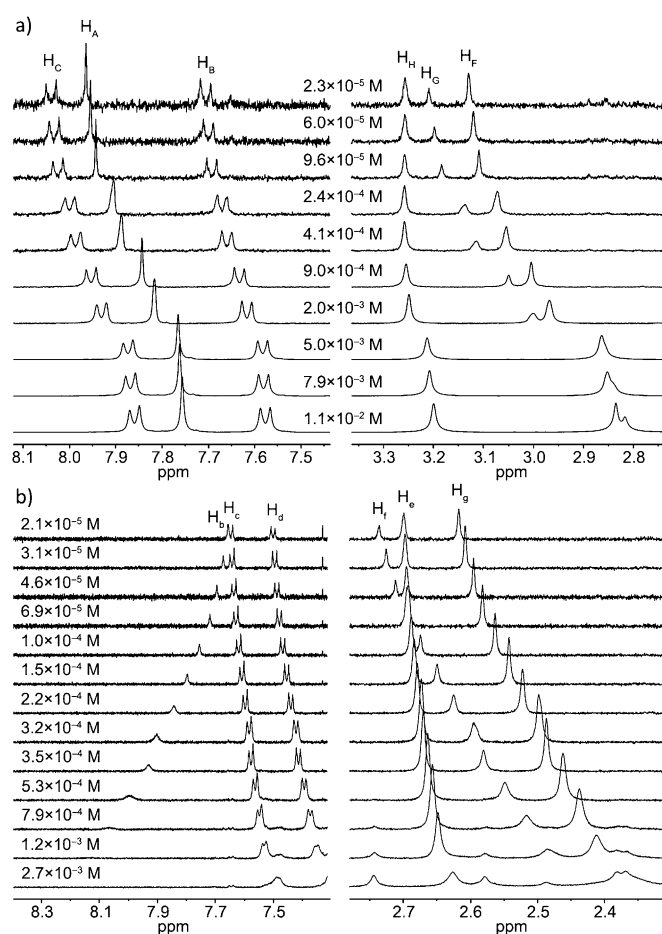


**Figure 3.** Concentration-dependent <sup>1</sup>H NMR spectroscopy of: a) **1** (400 MHz, 298 K, [D<sub>14</sub>]MCH), and b) **2** (500 MHz, 298 K, CCl<sub>4</sub>/CD<sub>2</sub>Cl<sub>2</sub> 9:1, v/v).

terms of both sufficiently sharp NMR signals and significant chemical shifts upon aggregation (Figure 3 b). Similar to **1** in  $[D_{14}]MCH$ , the upfield shifts of the protons of both the aromatic rings ( $H_a$ ,  $H_c$  and  $H_d$ ) and BODIPY core ( $H_e$ ,  $H_f$  and  $H_g$ ) with increasing concentration suggest the presence of strong  $\pi$ - $\pi$  stacking interactions of the molecules. In addition, the downfield shift of the amide proton ( $H_b$ ) with increasing concentration is a clear indication of hydrogen bonding during the supramolecular polymerization. These results are in agreement with a cooperative self-assembly, as previously shown by UV/Vis and fluorescence studies.

Quantum chemical calculations (PBEh-3c/HF-3c+COSMO-RS)<sup>[25]</sup> were performed to better understand the influence of the linkers on the molecular organization. For this, monomer, dimer and tetramer structures for BODIPY derivatives of **1** and **2** with peripheral  $OC_{12}H_{25}$  groups omitted (**1'**/**2'**) were optimized. Dimerization of **1'** and **2'** gave free energies of aggregation lower than experimentally determined ( $-0.3 \text{ kcal mol}^{-1}$  for ester **1'** and  $-1.6 \text{ kcal mol}^{-1}$  for amide **2'**), indicating that the omitted alkoxy groups provide additional stabilization of the stacks of **1** and **2**. The formation of tetramers from **1'** is predicted to be endothermic ( $+5.5 \text{ kcal mol}^{-1}$ ), but exothermic from **2'** ( $-2.6 \text{ kcal mol}^{-1}$ ). Clearly, the amide hydrogen bonds provide additional (enthalpic) stabilization to the  $\pi$ -stack of **2'** over **1'**. The conformations of both tetramers (**1'**)<sub>4</sub> and (**2'**)<sub>4</sub> show a tilting of the peripheral aromatic groups upon oligomerization, which is more pronounced for one side of the stack than for the other one (Figure 4, and Figures S27 and S28 in the Supporting Information). Interestingly, this rotational displacement induces a larger helical pitch for the amide (**2'**)<sub>4</sub> than for the ester tetramer (**1'**)<sub>4</sub>, most likely to facilitate an optimal conformation of the amide groups for hydrogen bonding. On increasing the stack length, subsequent torsions of the aromatic cores induce a progressive helicity in the stack, which is in agreement with previous spectroscopic investigations.

The molecular lengths of **1'** and **2'** deduced by the calculations (3.5 nm) are in very good agreement with the diameter of the supramolecular polymers observed by AFM (Figure 5). These studies for aggregate solutions of both **1** ( $1 \times 10^{-3} \text{ M}$ ) and **2** ( $1 \times 10^{-4} \text{ M}$ ) in MCH on highly oriented pyrolytic graphite (HOPG) reveal the formation of fiber-like structures with a regular diameter of 3.6 nm and lengths of approximately 100 nm. As the length of the molecular core is only slightly smaller than the average diameter of the aggregates, a strong interdigitation of the dodecyl chains between neighboring fibers should exist, which is apparent in Figure 5.

## Conclusions

To sum up, by comparing the self-assembly of two new hydrophobic BODIPY dyes that only differ in the linking group (ester vs. amide) we have shed light on the influence of these groups on the dye arrangement and, in turn, on the supramolecular polymerization mechanism. Although both dyes self-assemble in an H-type fashion, the participation of cooperative  $\pi$ - $\pi$  and hydrogen bonding interactions impose a rotationally displaced dye organization for the amide-containing dye, whereas the

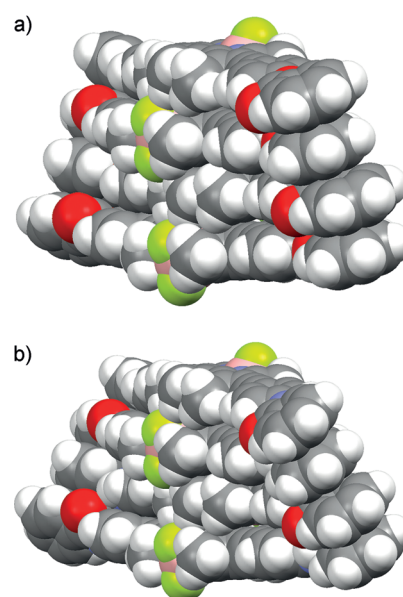


**Figure 4.** Optimized (HF-3c) conformation of: a) (**1'**)<sub>4</sub>, and b) (**2'**)<sub>4</sub>. Free energies of aggregation ( $\Delta G_{298}$  in cyclohexane) are  $+5.5 \text{ kcal mol}^{-1}$  for **1'** and  $-2.6 \text{ kcal mol}^{-1}$  for **2'**.

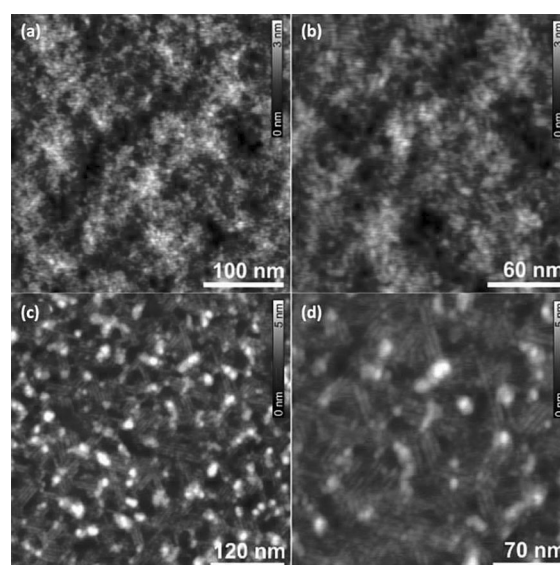


**Figure 5.** AFM images obtained by spin-coating of an aggregated solution of: a, b) **1**, and c, d) **2** on HOPG.

absence of hydrogen bonding in the ester derivative induces a non-cooperative parallel dye arrangement. Our results show that the interplay of various types of orthogonal noncovalent interactions is an efficient method to create ordered supramolecular polymers that are stabilized by cooperative effects. Our current efforts are focused on exploiting cooperative noncovalent forces in aqueous medium towards fluorescent BODIPY dye aggregates with potential application as drug delivery vehicles.

## Experimental Section

For detailed synthesis and characterization of the new compounds and target BODIPYs **1** and **2**, methods, additional experiments and images, see the Supporting Information.

## Acknowledgements

We thank the Alexander von Humboldt Foundation for financial support (Sofja Kovalevskaja Award).

**Keywords:** BODIPY dyes · cooperativity · non-covalent interactions · self-assembly · supramolecular chemistry

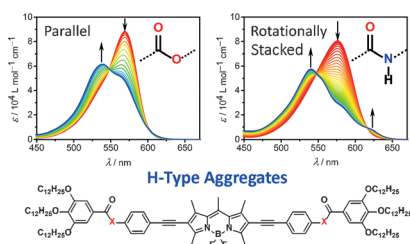
- [1] a) A. Das, S. Ghosh, *Chem. Commun.* **2016**, 52, 6860–6872; b) H. Frisch, P. Besenius, *Macromol. Rapid Commun.* **2015**, 36, 346–363; c) A. S. Tayi, A. Kaeser, M. Matsumoto, T. Aida, S. I. Stupp, *Nat. Chem.* **2015**, 7, 281–294; d) S. Yagai, *Bull. Chem. Soc. Jpn.* **2015**, 88, 28–58; e) R. D. Mukhopadhyay, A. Ajayaghosh, *Science* **2015**, 349, 241–242; f) S. S. Babu, V. K. Praveen, A. Ajayaghosh, *Chem. Rev.* **2014**, 114, 1973–2129; g) E. Busseron, Y. Ruff, E. Moulin, N. Giuseppone, *Nanoscale* **2013**, 5, 7098–7140; h) C. Kulkarni, S. Balasubramanian, S. J. George, *ChemPhysChem* **2013**, 14, 661–673; i) T. F. A. de Greef, M. M. J. Smulders, M. Wolffs, A. P. H. J. Schenning, R. P. Sijbesma, E. W. Meijer, *Chem. Rev.* **2009**, 109, 5687–5754.
- [2] a) P. A. Korevaar, S. J. George, A. J. Markvoort, M. M. J. Smulders, P. A. J. Hilbers, A. P. H. J. Schenning, E. W. Meijer, *Nature* **2012**, 481, 492–496; b) R. Thirumalai, R. D. Mukhopadhyay, V. K. Praveen, A. Ajayaghosh, *Sci. Rep.* **2015**, 5, 9842.
- [3] T. Aida, E. W. Meijer, S. I. Stupp, *Science* **2012**, 335, 813–817.
- [4] H. Kar, S. Ghosh, *Chem. Commun.* **2014**, 50, 1064–1066.
- [5] a) B. Isare, M. Linares, L. Zargarian, S. Femandjian, M. Miura, S. Motohashi, N. Vanthuyne, R. Lazzaroni, L. Bouteiller, *Chem. Eur. J.* **2010**, 16, 173–177; b) M. Roman, C. Cannizo, T. Pinault, B. Isare, B. Andrioletti, P. van der Schoot, L. Bouteiller, *J. Am. Chem. Soc.* **2010**, 132, 16818–16824.
- [6] a) A. Sikder, B. Ghosh, S. Chakraborty, A. Paul, S. Ghosh, *Chem. Eur. J.* **2016**, 22, 1908–1913; b) M. Yamauchi, T. Ohba, T. Karatsu, S. Yagai, *Nat. Commun.* **2015**, 6, 8936; c) H. Kar, D. W. Gehrig, F. Laquai, S. Ghosh, *Nanoscale* **2015**, 7, 6729–6736; d) J. S. Valera, J. Calbo, R. Gómez, E. Orti, L. Sánchez, *Chem. Commun.* **2015**, 51, 10142–10145; e) S. S. Babu, V. K. Praveen, K. K. Kartha, S. Mahesh, A. Ajayaghosh, *Chem. Asian J.* **2014**, 9, 1830–1840; f) J. M. Malicka, A. Sandeep, F. Monti, E. Bandini, M. Gazzano, C. Ranjith, V. K. Praveen, A. Ajayaghosh, N. Armaroli, *Chem. Eur. J.* **2013**, 19, 12991–13001; g) A. Das, M. R. Molla, B. Maity, D. Koley, S. Ghosh, *Chem. Eur. J.* **2012**, 18, 9849–9859; h) M. R. Molla, A. Das, S. Ghosh, *Chem. Eur. J.* **2010**, 16, 10084–10093.
- [7] a) F. Aparicio, S. Cherumukkil, A. Ajayaghosh, L. Sánchez, *Langmuir* **2016**, 32, 284–289; b) S. S. Babu, S. Prasanthkumar, A. Ajayaghosh, *Angew. Chem. Int. Ed.* **2012**, 51, 1766–1776; *Angew. Chem.* **2012**, 124, 1800–1810; c) P. Besenius, G. Portale, P. H. H. Bomans, H. M. Janssen, A. R. A. Palmans, E. W. Meijer, *Proc. Natl. Acad. Sci. USA* **2010**, 107, 17888–17893.
- [8] a) M. Yamauchi, S. Kubota, T. Karatsu, A. Kitamura, A. Ajayaghosh, S. Yagai, *Chem. Commun.* **2013**, 49, 4941–4943; b) T. Seki, A. Asano, S. Seki, Y. Kikkawa, H. Murayama, T. Karatsu, A. Kitamura, S. Yagai, *Chem. Eur. J.* **2011**, 17, 3598–3608.
- [9] H. Frisch, J. P. Unsleber, D. Lüdeker, M. Peterlechner, G. Brunklaus, M. Waller, P. Besenius, *Angew. Chem. Int. Ed.* **2013**, 52, 10097–10101; *Angew. Chem.* **2013**, 125, 10282–10287.
- [10] C. Rest, R. Kandanelli, G. Fernández, *Chem. Soc. Rev.* **2015**, 44, 2543–2572.
- [11] a) D. Sivaramakrishna, M. J. Swamy, *Langmuir* **2015**, 31, 9546–9556; b) M. Dirany, V. Ayzac, B. Isare, M. Raynal, L. Bouteiller, *Langmuir* **2015**, 31, 11443–11451; c) C. Kulkarni, K. K. Bejagam, S. P. Senanayak, K. S. Narayan, S. Balasubramanian, S. J. George, *J. Am. Chem. Soc.* **2015**, 137, 3924–3932; d) A. Ajayaghosh, V. K. Praveen, S. Srinivasan, R. Varghese, *Adv. Mater.* **2007**, 19, 411–415.
- [12] T. Kato, N. Mizoshita, K. Kishimoto, *Angew. Chem. Int. Ed.* **2006**, 45, 38–68; *Angew. Chem.* **2006**, 118, 44–74.
- [13] M. Chen, C. Wei, X. Wu, M. Khan, N. Huang, G. Zhang, L. Li, *Chem. Eur. J.* **2015**, 21, 4213–4217.
- [14] A. Treibs, F.-H. Kreuzer, *Liebigs Ann. Chem.* **1968**, 718, 208–223.
- [15] a) L. Yang, G. Fan, X. Ren, L. Zhao, J. Wang, Z. Chen, *Phys. Chem. Chem. Phys.* **2015**, 17, 9167–9172; b) H. Liu, J. Mack, Q. Guo, H. Lu, N. Kobayashi, Z. Shen, *Chem. Commun.* **2011**, 47, 12092–12094; c) Y. Tokoro, A. Nagai, Y. Chujo, *Tetrahedron Lett.* **2010**, 51, 3451–3454.
- [16] a) S. Choi, J. Bouffard, Y. Kim, *Chem. Sci.* **2014**, 5, 751–755; b) T. T. Vu, M. Dvorko, E. Y. Schmidt, J.-F. Audibert, P. Retailleau, B. A. Trofimov, R. B. Pansu, G. Clavier, R. Méallet-Renault, *J. Phys. Chem. C* **2013**, 117, 5373–5385; c) G. Fan, Y.-X. Lin, L. Yang, F.-P. Gao, Y.-X. Zhao, Z.-Y. Qiao, Q. Zhao, Y.-S. Fan, Z. Chen, H. Wang, *Chem. Commun.* **2015**, 51, 12447–12450; d) F. Camerel, L. Bonardi, M. Schmutz, R. Ziessel, *J. Am. Chem. Soc.* **2006**, 128, 4548–4549.
- [17] A. Florian, M. J. Mayoral, V. Stepanenko, G. Fernández, *Chem. Eur. J.* **2012**, 18, 14957–14961.
- [18] N. K. Allampally, A. Florian, M. J. Mayoral, C. Rest, V. Stepanenko, G. Fernández, *Chem. Eur. J.* **2014**, 20, 10669–10678.
- [19] a) Y.-Y. Ren, N.-W. Wu, J. Huang, Z. Xu, D.-D. Sun, C.-H. Wang, L. Xu, *Chem. Commun.* **2015**, 51, 15153–15156; b) D. S. Janni, M. K. Manheri, *Langmuir* **2013**, 29, 15182–15190; c) F. Wang, M. A. J. Gillissen, P. J. M. Stals, A. R. A. Palmans, E. W. Meijer, *Chem. Eur. J.* **2012**, 18, 11761–11770; d) K. C. Majumdar, B. Chattopadhyay, P. K. Shyam, N. Pal, *Tetrahedron Lett.* **2009**, 50, 6901–6905.
- [20] W. Qin, V. Leen, T. Rohand, W. Dehaen, P. Dedecker, M. Van der Auwerer, K. Robeyns, L. Van Meervelt, D. Beljonne, B. Van Averbeke, J. N. Clifford, K. Driesen, K. Binnemans, N. Boens, *J. Phys. Chem. A* **2009**, 113, 439–447.
- [21] a) F. C. Spano, C. Silva, *Annu. Rev. Phys. Chem.* **2014**, 65, 477–500; b) F. C. Spano, *Acc. Chem. Res.* **2010**, 43, 429–439; c) M. Kasha, H. R. Rawls, M. A. El-Bayoumi, *Pure Appl. Chem.* **1965**, 11, 371–392.
- [22] H. M. M. ten Eikelder, A. J. Markvoort, T. F. A. de Greef, P. A. J. Hilbers, *J. Phys. Chem. B* **2012**, 116, 5291–5301.
- [23] a) X.-Q. Li, V. Stepanenko, Z. Chen, P. Prins, L. D. A. Siebbeles, F. Würthner, *Chem. Commun.* **2006**, 3871–3873; b) F. Würthner, B. Hanke, M. Lysetska, G. Lambright, G. S. Harms, *Org. Lett.* **2005**, 7, 967–970.
- [24] C. Shao, M. Grüne, M. Stolte, F. Würthner, *Chem. Eur. J.* **2012**, 18, 13665–13677.
- [25] a) S. Grimme, J. G. Brandenburg, C. Bannwarth, A. Hansen, *J. Chem. Phys.* **2015**, 143, 054107; b) R. Sure, S. Grimme, *J. Comput. Chem.* **2013**, 34, 1672–1685.

Received: May 31, 2016

Published online on ■■■■■, 0000

## FULL PAPER

**Small strokes make big change:** Two new hydrophobic BODIPY dyes, which only differ in the linking group (ester vs. amide; see figure), were synthesized and fully characterized. Exchanging the ester linkages with amide groups is found to influence the mode of self-aggregation by tuning the isodesmic supramolecular polymerization to a cooperative process.



### Supramolecular Chemistry

A. Rödle, B. Ritschel, C. Mück-Lichtenfeld,  
V. Stepanenko, G. Fernández\*



**Influence of Ester versus Amide Linkers on the Supramolecular Polymerization Mechanisms of Planar BODIPY Dyes**

